PROCEEDINGS, 50th Workshop on Geothermal Reservoir Engineering
Stanford University, Stanford, California, February 10-12, 2025
SGP-TR-229

Illuminating geothermal reservoir structure: DAS microseismic reflection imaging at Utah FORGE

Yuanyuan Ma[1], Jonathan Ajo-Franklin[1], Michal Chamarczuk[1], Rosie Zhu[1], Jeremy Patterson[1], Ismael Vera Rodriguez[2], David Podrasky[2], Thomas Coleman[2] and Carlos Maldaner[2], and the FOGMORE@Utah FORGE team

[1] Rice University, Earth, Environmental and Planetary Sciences, Houston, Texas

[2] Silixa, Environment & Infrastructure, Missoula, Montana

ym50@rice.edu

Keywords: Fiber optic sensing, fracture imaging, microseismic, Utah FORGE

ABSTRACT

This study presents the latest insights into the reservoir structure and hydraulic fracture geometry at Utah FORGE obtained by using Distributed Acoustic Sensing (DAS) recorded microseismic data for subsurface reflection imaging. To monitor injection activities and evaluate reservoir response, two fibers were permanently deployed in wells [16B(78)-32] and [78(B)-32]. The DAS systems recorded abundant microseismic data during the 2023 circulation test, and the [16A(78)-32] and 16B dual-well stimulation sequences in 2024. We developed an imaging technique that leverages DAS microseismic events as imaging sources, with each fiber channel functioning as a receiver. We apply prestack Kirchhoff migration to each individual source following wavefield separation, then stack hundreds of sources to generate a 3D reflectivity volume. The developed imaging workflow produces a high-resolution map of the granitoid contact and, more importantly, reveals internal structures within the heart of the geothermal reservoir that have not been previously well described. By correlating well-log data, core analyses, and geological evidence, we identify a lithological interface located just below and nearly parallel to the granitoid contact. Key findings also reveal two potential natural fractures near the stimulation zone, visible prior to stimulation, which may accommodate the injected fluid, affecting the hydraulic fracturing efficiency. Those internal structures are hardly accessible by typical surface sources since the granite-alluvium interface of this region is strong and not easily penetrated by seismic waves. Time-lapse imaging of the hydraulic fracture is conducted and integrated with LF-DAS to construct a more comprehensive fracture geometry. In conclusion, the 3D fracture volume produced by DAS microseismic imaging deepens our understanding of geothermal reservoir dynamics, potentially enhancing geothermal exploitation strategies.

1. INTRODUCTION

The Frontier Observatory for Research in Geothermal Energy (FORGE) is an underground laboratory sponsored by the Department of Energy for developing, testing, and accelerating breakthroughs in Enhanced Geothermal Systems (EGS) technologies and advancing the uptake of geothermal resources around the world. Utah FORGE is located near Milford in Beaver County, Utah, on the western flank of the Mineral Mountains. The geothermal reservoir is dominated by hot (>175°C) crystalline granitoid, covered with overlying alluvial fill. The reservoir is tight, with low porosity and permeability; there is no evidence of modern hydrothermal fluid.

In support of the Utah FORGE project, high-resolution imaging of fractures and subsurface structure is required to understand the reservoir geology of this area and help identify a replicable pathway to EGS. While extensive efforts have been made to improve subsurface imaging and velocity inversion in this area, the intricate internal structure within the bedrock remains a significant challenge, primarily due to the limited data quality and the low imaging resolution. In particular, the west-dipping granite-alluvium interface of this region poses a unique obstacle, as the high reflectivity boundary reduces the seismic energy illuminating the EGS reservoir. To overcome this limitation and improve imaging quality, the use of seismic sources positioned below the granite-alluvium contact is critical.

FORGE site is well-instrumented for broad research projects about EGS. Among the wells drilled at FORGE, well [58-32] and [16A(78)-32] were used for stimulation, well [78(B)-32] and [16B(78)-32] were used for monitoring with optical fibers cemented behind the casing. Distributed Acoustic Sensing (DAS) has proven to be highly effective for a wide range of applications including geothermal reservoir monitoring (Lellouch et al., 2020; Ajo-Franklin et al., 2022), enabling direct surveillance of fracture geometry with low-frequency DAS (LF-DAS) cross-well strain and microseismic monitoring. Optical fibers can be km to tens of km long, providing high spatial resolution (below 1 m) monitoring of the entire well. The rich DAS microseismic wavefields facilitate detailed observation of subsurface wave propagation and the application of advanced imaging algorithms. Several attempts (Stanek et al., 2022; Ma et al., 2024) have explored the possibility of using DAS microseismic reflections for high-resolution hydraulic fracture imaging. The benefits of microseismic sources for imaging are similar to the resolution advantages provided by classical crosswell reflection imaging (Harris et al., 1995) except without the need to mobilize a powerful borehole source.

This study presents the latest insights into the reservoir structure and hydraulic fracture geometry at Utah FORGE by using DAS recorded microseismic data for subsurface imaging. The developed imaging workflow produces a high-resolution map of the granitoid contact and hydraulic fractures and, more importantly, reveals internal structures within the heart of the geothermal reservoir that have not been previously well described. These key findings enhance our understanding of geothermal potential and provide guidance for improving reservoir stimulation strategies.

2. METHODS

2.1 Data overview

In July 2023, circulation tests were conducted to investigate the hydraulic connection between the injector well 16A that was fractured in 2022, and the production well 16B (Figure 1). In April 2024, Utah FORGE conducted a commercial-scale stimulation sequence on both well 16A and 16B to create inter-well connectivity. Well 16A was hydraulically fractured in eight different stages and four stages of the production well 16B were then stimulated. To monitor injection activities, the FOGMORE@FORGE team (Fiber-Optic Geophysical Monitoring of Reservoir Evolution at the Utah FORGE Milford Site) permanently deployed a multi-mode optical fiber in the deviated well 16B, and the raw data were collected by a Silixa Carina interrogator unit (Figure 1). The vertical well 78B has a single-mode optical fiber cemented behind the casing interrogated with a Silixa iDAS v2 for monitoring. Both fibers (white dashed lines) are shorter than the wellbore due to field operations. The fiber optic sensing systems recorded microseismic, LF-DAS, Distributed Temperature Sensing (DTS), and Distributed Strain Sensing (DSS) data during the circulation test and the stimulation periods.

This study focuses on subsurface imaging and mainly uses the DAS microseismic data of well 16B that was collected using a gauge length of 10 m and a spatial interval of 1.0 m, with a frequency sampling rate of 1,000 Hz. The raw DAS microseismic data observed during the circulation and stimulation sequences have been properly processed (Vera Rodriguez et al., 2024) as shown in Figure 1. Thousands of microseismic events were located with a calibrated 3D velocity model, revealing multiple fracture planes that probably correspond with injection activities.

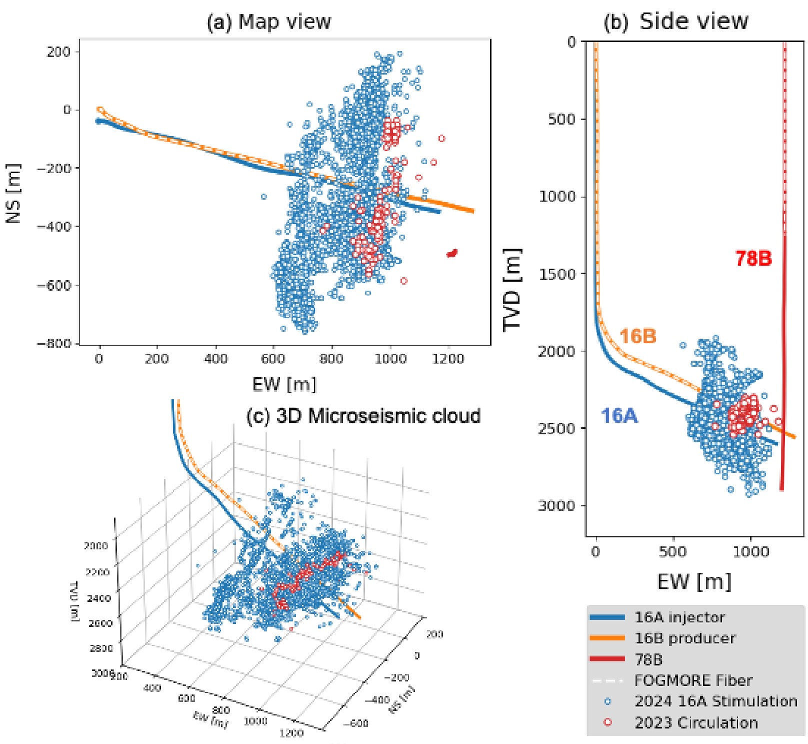

Figure 1: Well geometry of the Utah Forge project. (a) map view (b) side view (c) 3D visualization. Optical fibers are permanently installed in the deviated well 16B and the vertical well 78B. Microseismic clouds recorded during the circulation test in July 2023 and the stimulation of well 16A in April 2024 are shown (Rodriguez et al., 2024).

Figure 2 presents two microseismic examples recorded by the optical fiber in well 16B. In addition to direct P- and S-wave arrivals, the microseismic wavefields exhibit abundant reflected S-waves with linear moveout and strong amplitude, which indicates the presence of nearby induced fractures or structure with strong velocity changes (Ma et al., 2024). In the microseismic wavefield recorded during the circulation test (prior to stimulation, Figure 2a), most of the reflections propagate toward the toe side (blue arrows), which are inferred to reveal mineralogical variations within the basement or pre-existing structure. The S-P converted phase at the granite-alluvium contact (at 1.25 km) is clearly visible and tracked even above the granite contact benefiting from the dense spatial resolution provided by DAS. Figure 2b shows an event recorded during well 16A stage 9. Four groups of left-dipping reflections propagating toward the heel side are observed (red arrows). They are highly possibly induced by newly generated hydraulic fractures of the well 16A stimulation, as the reservoir was stimulated only on the toe side. While reflected P-waves are also visible in some events, this study focuses on reflected S-phases for imaging subsurface structure and fracture as they are more commonly observed and have superior data quality.

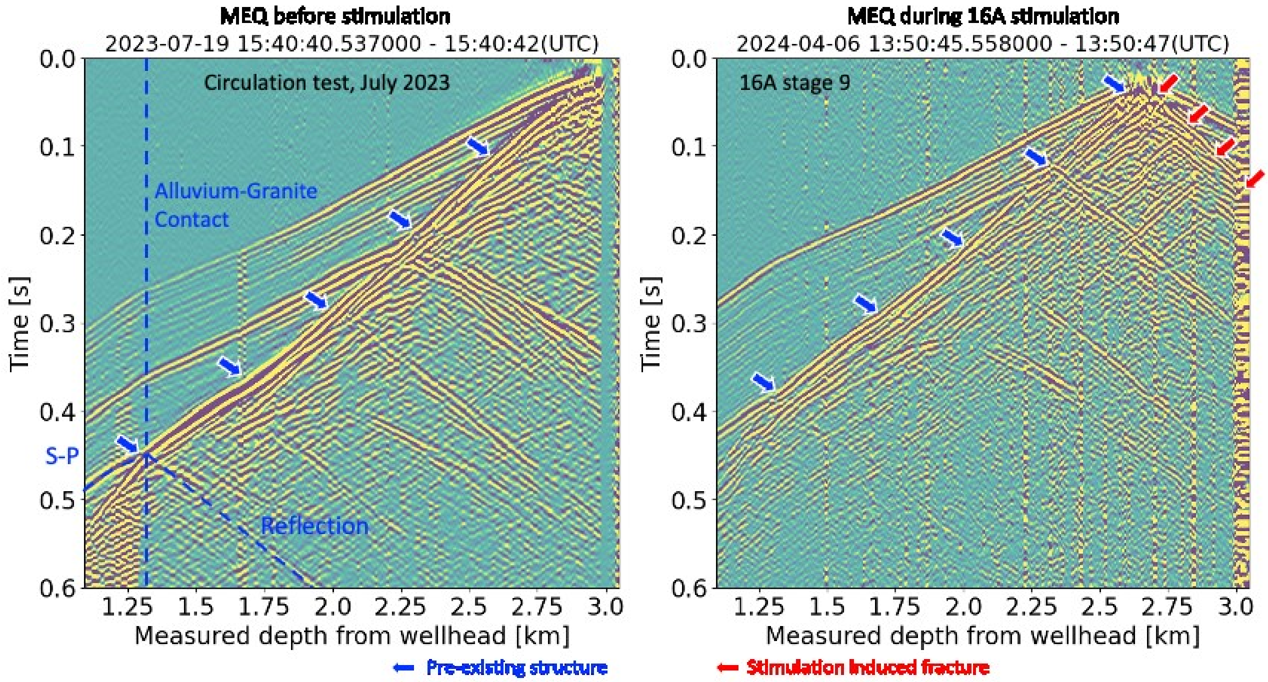

Figure 2: Examples of microseismic recorded by the FOGMORE fiber in well 16B, one during the circulation test in July 2023 (left) and one during the 16A stimulation in April 2024 (right). Blue arrows indicate reflected S-waves potentially originating from pre-existing subsurface structure, while red arrows highlight reflected S-waves associated with hydraulic fractures induced by the 16A stimulation sequence in April 2024.

2.2 Imaging methods

Before the imaging process, event selection is necessary to mitigate the potential impact of high noise levels in low signal-to-noise ratio (S/N) events on the final image quality. After analyzing the microseismic catalog, hypocenter uncertainties, and data quality, we selected over 1,700 events that exhibit imageable reflected S-waves on the DAS data. The event selection process only excludes sources with relatively weak reflections that are obscured by noise, thereby sacrificing data quantity for better imaging quality. However, considering that the microseismic cloud is located near the injection position and illuminates a similar subsurface area, the event selection does not decrease the imaging aperture that the raw data can provide.

The imaging strategy used in this study is to treat each microseismic event as a high-frequency seismic source, consider each fiber channel as a receiver, and apply a pre-stack Kirchhoff migration method for reflection imaging after wavefield separation. The proposed method requires accurate microseismic event locations, the optic fiber geometry, a well-calibrated velocity model, and DAS microseismic waveforms. The preprocessing of DAS microseismic data includes detrending, removing spikes, a median filter to attenuate common mode noise, and a bandpass filter between 10 and 150 Hz. Before migration, we apply an f-k filter for wavefield separation and mute the direct waves to extract reflected S-waves from the raw DAS data. Conventional 3D pre-stack Kirchhoff migration is applied separately to the wavefields propagating towards the toe and towards the heel of the lateral. We used a calibrated 3D S-wave velocity model (Rodriguez et al., 2024) to compute traveltime tables, then migrate microseismic traces on a $10 \times 10 \times 10$ m grid and output a 3D volume of potential reflectors. After imaging individual sources, reflectors from all selected microseismic events are stacked into a 3D reflectivity volume, enabling the delineation of multiple discrete reflectors. Selected events for stacking are determined based on the imaging target, as the geometry of microseismic sources is unevenly distributed and different sources may illuminate different parts of the reservoir. More details of the imaging methods have been introduced by Ma et al. (2024).

3. IMAGING RESULTS

3.1 Time-lapse hydraulic fracture imaging

One major objective of DAS microseismic reflection imaging is to characterize the fracture network induced by the stimulation sequence and monitor the fluid propagation. Figure 3 demonstrates the side view of the imaging results with a focus on the toe side. The time-lapse imaging results are generated by migrating only heel-ward reflections (marked by red arrows in Figure 2b) and stacking multiple microseismic sources stage by stage. The stacking strategy by stage is chosen to monitor fracture generation as the stimulation activities continue. The frac hits interpreted from LF-DAS data recorded during well 16A stimulation are marked by cyan diamonds.

Although certain imaging artifacts are visible due to a very narrow migration aperture provided by the geometry, the imaging results successfully present clear fracture features consistent with the LF-DAS, which is a promising outcome. Comparing the imaging results of stage 7, 8, and 9 in Figure 3, hydraulic fractures are observed to initiate and propagate from the toe to the heel as injection activities progress. Fractures from earlier stages remain visible in the imaging of the current stimulation stage, indicating that the proppant holds effectively and the fractures stay open and conductive, as the visibility of reflections requires a sufficient impedance contrast provided by fluid-filled fractures. For example, the reflectors from stage 7 appear relatively weaker than the new reflector generated in stage 8 but remain recognized (Figure 3b). Similarly, the reflector from stage 6 is visible in the imaging results of stage 7 (Figure 3a). Stages 3R to 6 of well 16A stimulation created fracture hits at a similar measured depth near the fiber end, as evidenced by the LF-DAS data (Ajo-Franklin et al., 2024). Consequently, only one strong fracture is imaged by the reflections for stage 3R to 6. Figure 3c illustrates the imaging results for stage 9 with optimized event selection. While this approach sacrifices some clarity, it preserves the majority of the reflection information, allowing all reflectors from prior stages to remain visible. The dipping angle of the imaged hydraulic fractures suggests that fluid propagation is influenced not only by the local stress field but also by pre-existing features. This aspect will be explored further in section 3.2.

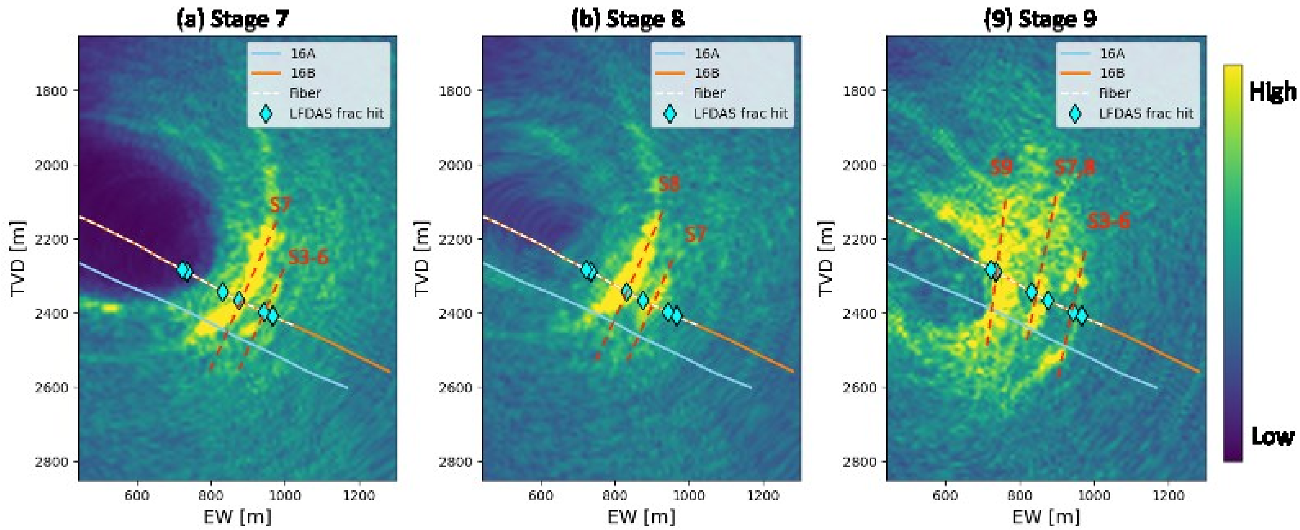

Figure 3: Time-lapse imaging of hydraulic fractures from stage 6 to stage 9 of well 16A stimulation.

3.2 Regional structure and natural fracture

Although the granitoid geothermal reservoir at Utah FORGE has been generally considered homogeneous, recent evidence suggests that natural fractures or structures exist within it and may influence the reservoir response to stimulation. Figure 4 illustrates examples of stage 8 and stage 9 where pre-existing natural fractures may affect the fluid path and fracture geometry. To better understand the subsurface structure and the mechanism, we merged the reflection imaging results of stages 8 and stage 9, and integrated them with microseismic clouds, LF-DAS data, and injection data, as shown in Figure 4. The LF-DAS data recorded by well 16B during stage 8 stimulation is displayed in Figure 4a, with the relative injection position and the observed frac hit clearly marked. Cross-well strain data reveals that fluid propagates upward over 200 m, creating a heart-shaped ‘fracture’ opening response. This pattern suggests that a pre-existing natural fracture or fault may be influencing and accommodating the injected fluid. The reflection imaging results (Figure 4b) show a west-dipping hydraulic fracture (marked by the red dashed line) generated by stage 8 injection, which aligns with the microseismic clouds and the frac hit (cyan diamond). More importantly, two steeply dipping small faults are imaged (blue dashed line). One fault (Fault 1) appears consistent with the strong heart-shaped frac hit shown in the LF-DAS and connects with microseismic clouds of both stage 8 and 9. The second fault, located further west (Fault 2), was not activated by the stimulation activities but is still revealed by the reflection imaging. Injection fluid may be transported from the injection position (pentagon) through deep corridors below well 16A at a depth of approximately 2500 m, then captured by the pre-existing fault structure, triggering intense microseismic activity. While further analysis is required to confirm this hypothesis, the evidence of both microseismic clouds and reflection imaging strongly supports it.

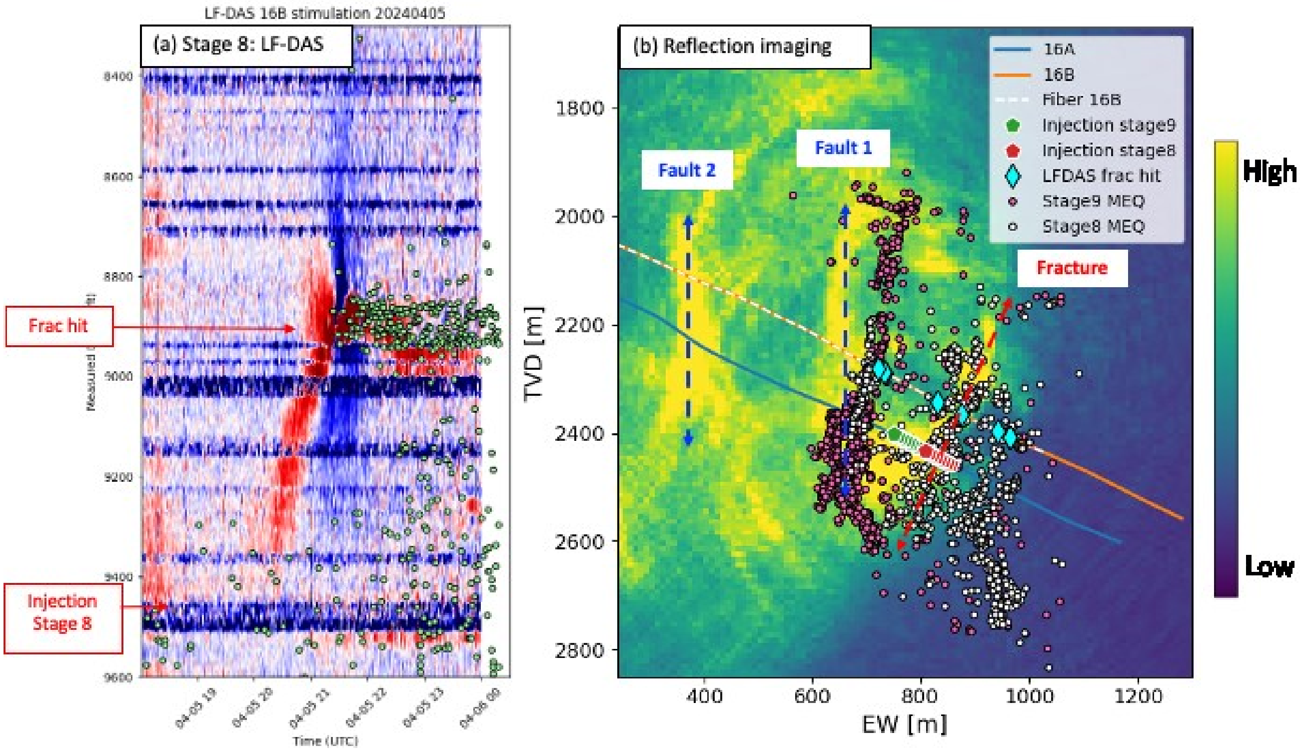

Figure 4: Integration of reflection imaging with MS cloud and LF-DAS to understand geothermal response, showing pre-existing structure affect fluid propagation. (a) LF-DAS data of stage 8 (b) Internal structure and hydraulic fracture imaged by microseismic reflections during 16A stage 8 and stage 9.

In addition to mapping hydraulic and natural fractures, DAS microseismic reflection imaging also shows promise for revealing hidden large-scale structures at the Utah FORGE site. To obtain a more complete image of the subsurface, we included the DAS data recorded by the Delano well (courtesy of Fervo Energy), performed reflection imaging, and combined these results with the imaging from well 16B. Delano is a deep vertical well located approximately 1.2 km southwest of the Utah FORGE site (Figure 5), therefore providing additional illumination for subsurface imaging.

Figure 5 a shows the side view of the merged imaging volume, presenting the regional alluvium-granite interface inferred by the imaged reflector, which is consistent with the velocity model built by a surface nodal array (Zhang and Pankow, 2021) and the structure imaging by converted phases (Kim et al., 2023) but provides a higher resolution. Below the interface, two small reflectors are imaged and show similar dipping angles with the granite contact. One possible explanation for those internal structures is lithology and mineralogy changes within the granite basement (Jones et al., 2024; Ma et al., 2024). These reflectors exhibit relatively lower gamma ray value than the surrounding rock, and seem to be related to the shift between ‘quartz-rich’ and ‘quartz-poor’ rock based on the X-ray diffraction (XRD) analysis of well cuttings, core, and outcrop samples from the Utah Forge site (Jones, 2021). Two vertical faults are further characterized and the corresponding reflections are visible on the raw data from both Delano and 16B. Those internal structures are hardly accessible by surface sources or receivers since the granite contact of this region is strong and not easily ‘penetrated’ by seismic waves. High-resolution imaging of those internal structures could provide insight into the understanding of the EGS reservoir and optimize stimulation and production. Figure 5b shows the map view of the merged imaging volume, overlying with the Mineral Mountain West Faul Zone (MMWF, Knudsen et al., 2019). The two vertical faults share a similar north-south azimuth (red dashed lines), which may indicate the MMWF system extends into basement rocks where they might tap hydrothermal fluids, while further independent analysis is required to validate the hypothesis.

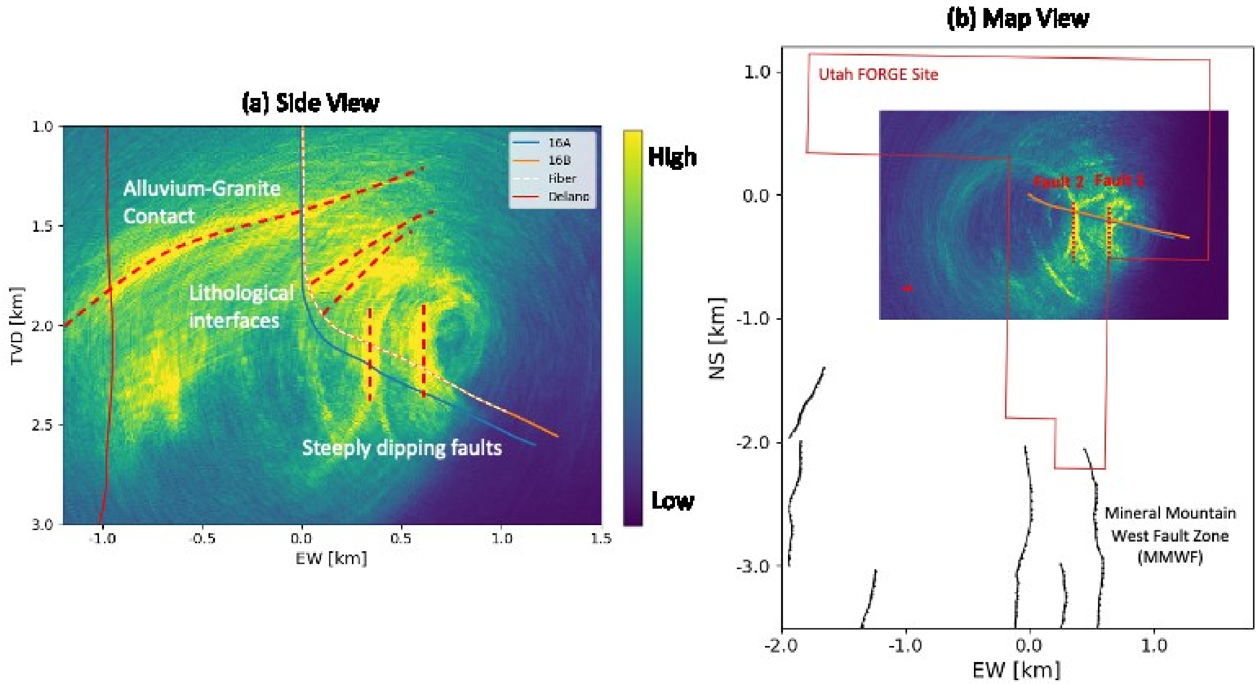

Figure 5: Internal structure at Utah FORGE revealed by DAS microseismic reflection imaging, including the regional alluvium-granite contact, the lithology interfaces, and potential fault zones.

4. CONCLUSIONS

This study highlights the potential of DAS microseismic reflection imaging for high-resolution subsurface characterization and fracture mapping to monitor geothermal reservoirs. By leveraging DAS and microseismic sources, the developed workflow revealed intricate subsurface structures, including the granitoid contact, natural and hydraulic fractures, and internal lithology changes within the bedrock at the Utah FORGE site. These findings provide critical insights into understanding geothermal reservoir dynamics, improving EGS efficiency and sustainability, and enhancing the optimization of EGS exploitation. Future work will focus on refining imaging techniques, integrating with multi-disciplinary data, and extending applications to a broader range of geothermal systems.

ACKNOWLEDGMENTS

This project is supported by DOE EERE Geothermal Technologies Office to Utah FORGE and the University of Utah under Project DE-EE0007080 Enhanced Geothermal System Concept Testing and Development at the Milford City, Utah Frontier Observatory for Research in Geothermal Energy (Utah FORGE) site.

REFERENCES

Ajo-Franklin, J., Chamarczuk, M., Ma, Y., Kim, J., Coleman, T., Maldaner, C., Rodriguez, I., V., Broman, B., Podrasky, D., Correa, J., Wood, T., J., Robertson, M., Freifeld, B., Becker, M., Ghassemi, A. (2024). Distributed Fiber-Optic Sensing Deployment in a Deep EGS Production Well at Utah FORGE: Preliminary Results and Lessons Learned. IMAGE 2024, Houston.

Harris, J. M., Nolen-Hoeksema, R. C., Langan, R. T., Schaack, M. V., Lazaratos, S. K., and Rector, J. W., 1995. High-resolution crosswell imaging of a west Texas carbonate reservoir: Part 1—Project summary and interpretation. GEOPHYSICS 60: 667-681. https://doi.org/10.1190/1.1443806

Jones, C., 2021. Energy and Geoscience Institute at the University of Utah. Utah FORGE Well 16A(78)-32 X-ray Diffraction Data [data set]. Retrieved from https://dx.doi.org/10.15121/1811309.

Jones, C., Simmons, S. and Moore, J. N., 2024. Geology of the Utah Frontier Observatory for Research in Geothermal Energy (FORGE) Enhanced Geothermal System (EGS) Site, Geothermics, Volume 122, 2024. https://doi.org/10.1016/j.geothermics.2024.103054.

Kim, J., J., Ajo-Franklin, T., Shadoan, V., Sobolevskaia, J., Correa, and B., Freifeld, 2023, A dense linear array for passive seismic imaging of geothermal structural features: The FOAL experiment at Utah FORGE, SEG Technical Program Expanded Abstracts: 935-939. https://doi.org/10.1190/image2023-3913927.1

Knudsen, T., Kleber, E., Hiscock, A., and Kirby, S.M., 2019, Quaternary geology of the Utah FORGE site and vicinity, Millard and Beaver Counties, Utah, in Allis, R., and Moore, J.N., editors, Geothermal characteristics of the Roosevelt Hot Springs system and adjacent FORGE EGS site, Milford, Utah: Utah Geological Survey Miscellaneous Publication 169-B, 21 p., 2 appendices, https://doi.org/10.34191/MP-169-B.

Ma, Y., J., Ajo-Franklin, A., Nayak, X., Zhu, J., Correa, 2024, DAS microseismic reflection imaging for hydraulic fracture and fault zones mapping, Geophysics, vol 89, no. 4.

Ma, Y., Ajo-Franklin, J., Chamarczuk, M., Patterson, J., Rodriguez, I., V., Podrasky, D., Coleman, T., Maldaner, C. (2024). Illuminating geothermal reservoir structure: DAS microseismic imaging at Utah FORGE. IMAGE 2024, Houston.

Staněk, F., Jin, G., and Simmons, J., 2022. Fracture imaging using DAS-recorded microseismic events. Front. Earth Sci. 10:907749. doi: 10.3389/feart.2022.907749.

Zhang, H., and K. L. Pankow, High-resolution Bayesian spatial autocorrelation (SPAC) quasi-3-D Vs model of Utah FORGE site with a dense geophone array, Geophysical Journal International, Volume 225, Issue 3, June 2021, Pages 1605–1615, https://doi.org/10.1093/gji/ggab049

Vera Rodriguez, I., Wolpert, J., Podrasky, D., Coleman, T., Maldaner, C., Ma, Y., Chamarczuk, M., Ajo-Franklin, J. and Becker, M.: DAS microseismic monitoring results from the July 2023 circulation tests at the Utah FORGE geothermal underground laboratory, SEG/AAPG International Meeting for Applied Geoscience & Energy 2024, Expanded Abstracts (2024).